Available online at www.sciencedirect.com
ScienceDirect
Catalysis Today 131 (2008) 111–117
CATALYSIS TODAY
www.elsevier.com/locate/cattod

Synthesis and characterization of cobalt–molybdenum bimetallic carbides catalysts

Xiao-Hui Wang [a,b], Ming-Hui Zhang [a,*], Wei Li [a], Ke-Yi Tao [a]

[a] Institute of New Catalytic Materials Science, College of Chemistry, Nankai University, Tianjin 300071, PR China
[b] Department of Stem Cell and Regenerative Medicine, Beijing Institute of Transfusion Medicine, Beijing 100850, PR China

Available online 26 November 2007

Abstract

Co_3Mo_3C, Co_6Mo_6C and MCM41-supported Co_3Mo_3C catalyst are prepared by a simple one-step thermal decomposition method without the conventional temperature-programmed carburization. The resultant carbides are characterized by X-ray diffraction (XRD), scanning electron microscopy (SEM), high-resolution transmission electron microscope (HRTEM) and BET surface area measurements. The as-prepared Co_3Mo_3C/MCM41 catalyst exhibits good performance in both probe reactions of hydrodesulfurization (HDS) and hydrodenitrogenation (HDN), which proves the one-step decomposition method to be an effective route for the preparation of bimetallic carbide catalyst.

Keywords: Bimetallic carbide; HMT; Catalyst; HDS; HDN

1. Introduction

In recent years, because the allowable amount of emissions, such as SO_x, NO_x and aromatics from the combustion of fuels has been greatly decreased, petroleum refining industry is facing real challenges. Co(Ni)Mo(W)/Al_2O_3 catalysts have been commercially used for more than half a century in petroleum refining industry due to their reliable activity and thermal resistance. In order to meet the new regulation, it is essential for the refiners to develop novel catalytic materials for the production of high-purity and clean fuels.

Since the last decade, metal carbides have been expected to be one of the potential substitutes to conventional refining catalysts. In this regard, interstitial molybdenum-based carbides have attracted much attention of catalysis researchers in hydrogen-involved reactions, such as hydrogenolysis, hydrogenation, dehydrogenation, isomerization, hydrodesulfurization (HDS), hydrodenitrogenation (HDN), ammonia synthesis, etc. [1–16]. However, most research findings focused on the outstanding functions and new preparation methods of monometallic molybdenum carbides, rather than those of bimetallic molybdenum-based carbides, despite the potential advantages of attaining multi-functional catalysts from bimetallic ones. To the best of our knowledge, it could be ascribed to inexperience in the preparation of bimetallic carbides, which generally included the temperature-programmed nitridation of corresponding oxides and the subsequent carburization of the nitrides.

The prime study concerning the preparation and characterization of cobalt-molybdenum bimetallic carbides was reported by Newsam et al. [17]. They successfully synthesized $Co_6Mo_6C_2$ (Co_3Mo_3C) as well as Co_6Mo_6C with $Co(en)_2MoO_4$ as precursor by a two-stage reaction method, and the structures of these carbides were firstly confirmed by Rietveld analyses of powder neutron diffraction data. In recent years, Bussell's group synthesized the bulk and alumina supported Co_3Mo_3C through a temperature-programmed nitridation and subsequent topotactic carburization route [18]. The thiophene HDS property of as-prepared catalysts was investigated and compared with those of the corresponding nitride and oxide [8]. Although such a multi-staged method based on the temperature-programmed procedure was proved to be effective for the synthesis of bulk and supported Co_3Mo_3C [18,19], Co_6Mo_6C could not be synthesized by this method and no other synthesis route has been proposed since 1988 [17]. Besides, another carburization approach for the preparation of Co-Mo carbides was presented by Xiao et al., who used oxidic precursor instead of nitride and operated the carburization under the flow of C_2H_6/H_2 mixture [20]. This method resulted

* Corresponding author. Tel.: +86 22 23507730; fax: +86 22 23507730.
E-mail address: Zhangmh@nankai.edu.cn (M.-H. Zhang).

0920-5861/$ – see front matter
doi:10.1016/j.cattod.2007.10.070

in a series of carbides, namely $Co_{0.2}Mo_{0.8}C_x$, $Co_{0.33}Mo_{0.67}C_x$, $Co_{0.4}Mo_{0.6}C_x$ and $Co_{0.5}Mo_{0.5}C_x$. The authors also tested their activities toward HDN of pyridine and concluded that all the bimetallic catalysts were more stable and active than pure molybdenum carbide and corresponding bimetallic nitride, oxide and sulfide ($CoMoN_x$, $CoMoO_x$ and $CoMoS_x$) [21,22]. On the other hand, Liang et al. developed a carbothermal hydrogen reduction method for the preparation of Co–Mo carbide [23] as well as nanostructured β-Mo_2C [24] and W_2C [25]. In this novel synthesis route, activated carbon material was used as carbon source and support. However, it was difficult to prepare bimetallic Co–Mo carbide loading on other supports for catalytic applications through this method. So the aim of this study is to propose a novel and simple method to prepare bulk and supported Co–Mo carbides and to evaluate the catalytic activity of as-prepared catalysts.

Hexamethylenetetramine (HMT), an organic compound containing both C, N elements, has been utilized as molybdate ion ligand and reducing agent to prepare Mo_2N as well as bimetallic Ni_2Mo_3N and Co_3Mo_3N by a one-step decomposition method [26,27]. Recently, bulk and alumina supported β-Mo_2C has also been successfully synthesized by the HMT-based method in our previous work [28]. In the current study, two phases of cobalt–molybdenum bimetallic carbides, Co_3Mo_3C and Co_6Mo_6C, were both prepared by the HMT-based one-step thermal decomposition method. The microstructures and properties of the bulk carbides were investigated and compared by XRD, BET, SEM and HRTEM characterizations. With respect to extend the simple synthesis route to catalysis research, the MCM41 zeolite was employed as a steady support, due to its good thermal stability, high surface area, and large adsorption capacity for organic molecules. To testify the catalytic performance of the resultant Co_3Mo_3C/MCM41 catalyst, the HDS of dibenzothiphene (DBT) and 4,6-dimethyldibenzothiophene (DMDBT) and HDN of 3-methylpyridine were used as two probe reactions. In general, this method is proved to be successful and has the potential to be a general and convenient route to prepare Co-Mo bimetallic carbide on various supports.

2. Experimental

2.1. Synthesis

2.1.1. Synthesis of Co_3Mo_3C

Commercially available solvents and reagents were used in the whole procedure. A precursor to pure phase Co_3Mo_3C was prepared by dissolving $Co(CH_3COO)_2{\cdot}4H_2O$, $(NH_4)_6Mo_7O_{24}{\cdot}4H_2O$ and HMT with a mole ratio of 7:1:37 in 15% $NH_3{\cdot}H_2O$ solution under stirring. The molar ratio of the above compounds was confirmed by trial and error with the fixed atomic ratio of Co/Mo = 1. The magenta solution was evaporated at room temperature to dryness to obtain the magenta slurry. The resulting material was dried under vacuum at 353 K for 6 h and then crushed to get a fine powder. Co_3Mo_3C was synthesized by thermal decomposition of the as-prepared powder precursor in a stainless steel reactor under a flow of argon (99.99%). In the thermal treatment process, the system was heated to 1023 K at a rate of 10 K min^{-1} and held at this temperature for 2 h. After the heat treatment, the samples were cooled to room temperature naturally under argon and passivated in a flow of 1% (v/v) O_2/N_2 for 2 h.

2.1.2. Synthesis of Co_6Mo_6C

A mixed-salt precursor to bulk Co_6Mo_6C was prepared by dissolving $Co(NO_3)_2{\cdot}6H_2O$, $(NH_4)_6Mo_7O_{24}{\cdot}4H_2O$ and HMT with a mole ratio of 7:1:23 in 15% $NH_3{\cdot}H_2O$ solution under stirring, then evaporating to dryness. The subsequent steps were carried out as described above for the synthesis of Co_3Mo_3C.

2.1.3. Synthesis of Co_3Mo_3C/MCM41

The Co_3Mo_3C/MCM41 catalyst with the theoretical loading of 16.7 wt.% Co_3Mo_3C was prepared by incipient wetness impregnation of finely ground MCM41 with the above described homogenous solution. The subsequent procedure followed that of the bulk sample through the thermal decomposition method.

For comparison purpose, 17 wt.% Co_3Mo_3C/MCM41 was also synthesized from the supported bimetallic nitride precursor by the conventional temperature-programmed carburization method under flowing 20 mol.% CH_4/H_2 mixture at a VHSV (volume hourly space velocity) of 6000 h^{-1}. The Co_3Mo_3N/MCM41 precursor was prepared by ammonolysis of supported metal oxides, which obtained by incipient wetness impregnation of MCM41 using aqueous solutions of $(NH_4)_6Mo_7O_{24}{\cdot}4H_2O$ and $Co(CH_3COO)_2{\cdot}4H_2O$ followed by drying and calcination in air. The temperature of nitridation process was increased in two steps: rapidly from room temperature to 623 K (at 6 K min^{-1}), and then slowly from 623 to 973 K (at 1 K min^{-1}). The temperature was then held at 973 K for 2 h. The sample was cooled in flowing NH_3 and passivated for 2 h. Before carburization, the nitride intermediate was reduced under H_2 flow at 673 K for 3 h to remove the passivation layer. Subsequently, the system was heated to 923 K at the ramping rate of 5 K min^{-1} under carburizing agent CH_4/H_2, and then cooled and passivated in 1% (v/v) O_2/N_2 for 2 h to avoid strong bulk oxidation.

2.2. Characterization

X-ray diffraction (XRD) patterns of the samples were acquired on a Rigaku D/max-2500 powder diffractometer employing Cu-Kα source (λ = 1.5418 Å, 40 kV, 40 mA). The powder samples were mounted on a silicon plate for XRD characterization. The carbon analysis of the samples was carried out with an Elementar Vario EL elemental analyzer. The particle size and morphology of the samples were characterized using a LEO 1530VP scanning electron microscopy (SEM). The samples were covered by a thin film of gold for better image definition. A JEM-2010FEF high-resolution transmission electron microscope (HRTEM) equipped with an EDX system (EDAX) operating at 200 kV was conducted to observe the morphology and microstructure of the bulk samples. BET surface areas of the samples were determined from N_2 BET

isotherms by Surface Area and Pore Analyzer (Quantachrome NOVA 2000e) apparatus.

2.3. Catalytic tests

The HDN and HDS reactions were separately performed in a tubular fixed-bed reactor under H_2 pressure of 3.0 MPa at several temperatures. The MCM41 supported carbide catalyst (weight = 0.35 g, volume = 1.0 ml for both reactions, grain size 0.38–0.83 mm) and quartz sand were mixed at a volume ratio of 1:4. The hydrogen flow of total pressure was controlled by a mass flow controller and a back-pressure regulator. Prior to evaluation, both catalysts were pretreated under a H_2 flow of 30 ml/min at 673 K for 3 h at atmospheric pressure. Then the temperature of the system was cooled to the reaction temperature and the pressure was increased to 3.0 MPa.

The HDN reaction of 3-methylpyridine was performed at 523, 543, 563, 583 and 603 K. After the temperature was cooled to 523 K, a cyclohexane solution of 3-methylpyridine (1.0 wt.%) was fed into the reactor by a high-pressure pump and the system was stabilized at this temperature for 4 h. The H_2 flow rate and the liquid feed rate were respectively maintained at 150 ml/min and 15.0 ml/h, and the H_2/feed ratio of 600 was determined. The liquid product was collected at a 1 h interval and analyzed by gas chromatography with a flame ionization detector. The HDN activity was calculated by the conversion of 3-methylpyridine.

In the HDS reaction, DBT and 4,6-DMDBT were simultaneously chosen as model compounds to investigate the deep HDS performance on bimetallic carbide catalysts. As described above, the system was stabilized at the first temperature of 553 K for 4 h with the liquid feed containing 0.20 wt.% 4,6-DMDBT and 0.30 wt.% DBT in decalin under a H_2 flow of 50 ml/min. The liquid feed rate was kept at 5.0 ml/min and the ratio of H_2/feed was set to 600. The liquid products at 573 and 593 K were collected and analyzed at a 1 h interval. The HDS activity was calculated by the conversion of DBT and 4,6-DMDBT.

3. Results and discussion

3.1. The bulk Co–Mo bimetallic carbides

The XRD patterns of as-prepared bulk Co_3Mo_3C and Co_6Mo_6C and standard data [17] from JCPDS database are shown in Fig. 1. Several heat treatment operations under different conditions were performed in order to determine the appropriate conditions such as the content of HMT in the precursor, the final temperature, holding time and ramping rate to obtain pure phase product. Inspection of Fig. 1a indicates little difference could be found between the pattern and the standard data in the locating position and the relative intensity, which documents that pure phase Co_3Mo_3C has been successfully prepared by this one-step thermal decomposition method. Considering the preparation of Co_3Mo_3N through the HMT-based method in our previous report [27], it is worth noting that low content of HMT (14:2:25) in the precursor leads to bimetallic nitride, while high content of HMT (7:1:37) results in bimetallic carbide. In other words, it is the excessive

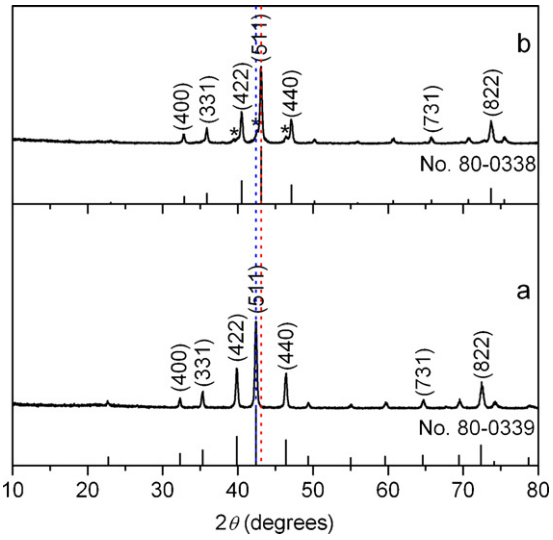

Fig. 1. XRD patterns and standard data of Co_3Mo_3C and Co_6Mo_6C. (a) Co_3Mo_3C and (b) Co_6Mo_6C. The asterisks represent the impurities.

HMT that works on the phase transformation from nitride to carbide. In fact, in the preparation of monometallic β-Mo_2C through this HMT-based method [28], investigation of the formation process has revealed that β-Mo_2C was formed by the carburization of γ-Mo_2N with the carbon-enriched pyrolysate yielded from decomposition of excess HMT in the precursor. In the case of Fig. 1b, because the metal atom arrangement and the type of crystal lattice (*Fd3m*) of Co_6Mo_6C are the same as Co_3Mo_3C, only little shifts of 2θ values could be observed for all reflection peaks in comparison with Fig. 1a. The most intense seven peaks of the b pattern locating at $2\theta = 43.08$, 40.50, 47.10, 73.72, 35.84, 65.74, 32.80° match quite well with the standard data of face-centered cubic Co_6Mo_6C [17]. It confirms that Co_6Mo_6C has been prepared by this heat treatment route, except for a small quantity of Co_3Mo_3C and β-Mo_2C impurities, marked as asterisks in the figure. In addition, according to elemental analysis results, the carbon contents of the samples of Fig. 1a and b are determined to be 2.39 and 1.35 wt.%, respectively. Considering the theoretic carbon contents of Co_3Mo_3C and Co_6Mo_6C are 2.52 and 1.27 wt.%, the compositions of as-prepared samples coincide well with their molecular formulas. The BET surface areas of the bimetallic carbides synthesized by our new approach are measured, which are 14.61 m^2/g for Co_3Mo_3C and 7.09 m^2/g for Co_6Mo_6C. Further synthesis optimization and purification to prepare single phase Co_6Mo_6C have been performed, but the products are in all cases impure. With the holding time extended to 4 h (XRD pattern not given), an increase in intensity of the reflection peaks indexed to β-Mo_2C phase is observed besides those of Co_3Mo_3C and metal Co impurities. Furthermore, the details of the conditions in our new approach are likely to be critical and the proper conditions to prepare single phase Co_6Mo_6C are difficult to access.

The SEM micrographs of the as-prepared bimetallic carbides, Co_3Mo_3C and Co_6Mo_6C, are respectively given in Fig. 2a and b. The particle sizes measured by SEM are denoted in the figure. Co_3Mo_3C presents as irregular particles with a

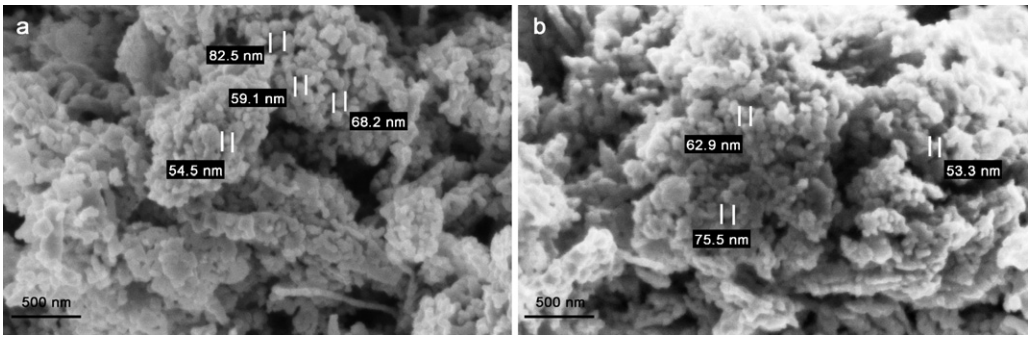

Fig. 2. SEM images of the bulk samples. (a) Co_3Mo_3C and (b) Co_6Mo_6C.

size of about 55–80 nm, accumulating on a matrix of large sandwich agglomerates. Because of the same preparing conditions except for different HMT content, Co_6Mo_6C sample presents the similar morphology, particle size and size distribution to those of Co_3Mo_3C.

Fig. 3 shows the HRTEM micrographs together with the EDX analysis of the bulk bimetallic carbides. In Fig. 3a, *d*-spacing values of 0.639 and 0.391 nm, respectively corresponding to the (1 1 1) and (2 2 0) crystallographic planes are yielded, which are in good agreement with the XRD pattern for single-phase Co_3Mo_3C. Likewise, *d*-spacing value of 0.209 nm can be obtained from Fig. 3b, which is coincident with the most intense peak of the (5 1 1) crystallographic planes of Co_6Mo_6C based upon the data of the XRD result. Moreover, according to Fig. 3b, a nearly round-shaped crystallite of Co_6Mo_6C has the diameter of c.a. 35 nm, smaller than the particle size observed by SEM. EDX analysis of both a and b microregions indicates that the nanoparticles are consisted of Co, Mo, C and O elements. The results accord quite well with the expectation, in which the existence of oxygen element is due to the passivation process.

3.2. MCM41-supported Co_3Mo_3C catalyst

Since the impurities still remain in bulk Co_6Mo_6C as indicated above, the work on preparing supported Co_6Mo_6C has not been carried out. As shown in Fig. 4, the diffused peak of 4b located in the range of low 2θ value can be assigned to MCM41 support, and all the other peaks accord with those of Co_3Mo_3C. Thus, the MCM41 supported Co_3Mo_3C catalyst is successfully prepared by the one-step heat treatment from MCM4-supported mixed-salt precursor. The average crystalline size is calculated to be 19.7 nm by the full-width at half-maximum (fwhm) of the XRD peaks according to Scherrer's equation. Furthermore, the BET surface area of Co_3Mo_3C/MCM41 is measured to be 529.3 m^2/g. Comparing with the surface area of bulk MCM41 support (843.5 m^2/g), it demonstrates that the destruction of the MCM41 in this new method is not severe, and the reduced

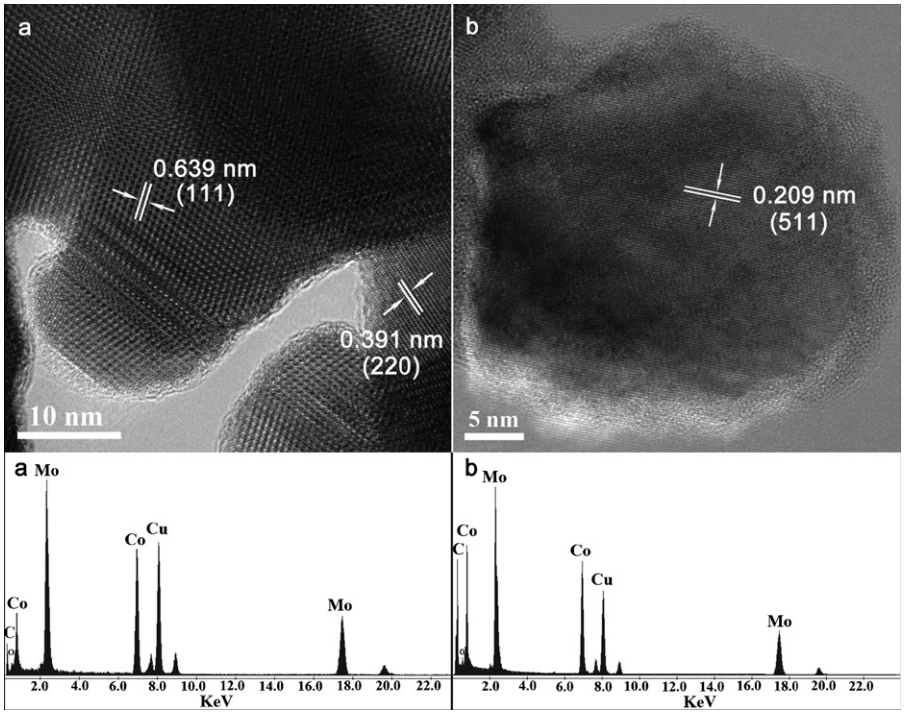

Fig. 3. HRTEM micrographs together with the EDX analyses of the microregions. (a) Co_3Mo_3C and (b) Co_6Mo_6C.

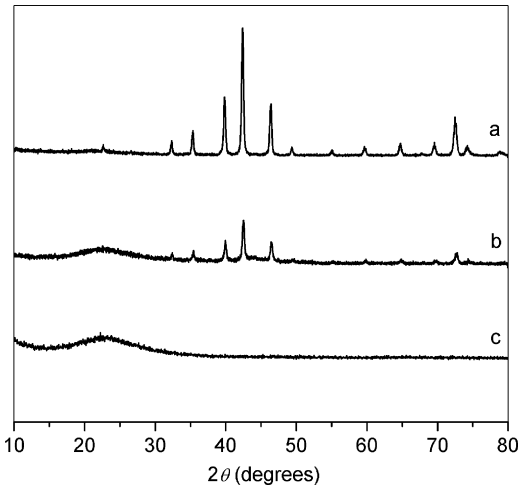

Fig. 4. XRD patterns of MCM41-supported catalysts. (a) Co_3Mo_3C, (b) Co_3Mo_3C/MCM-41 and (c) MCM-41.

surface area may be ascribed to the blockage of carbide on the support.

To estimate the particle size of the MCM41 supported Co_3Mo_3C catalyst prepared by the thermal decomposition method, TEM and HRTEM were carried out. Fig. 5a displays a typical TEM micrograph of Co_3Mo_3C nanoparticles loading on MCM41. It clearly shows that the particles have a narrow distribution with the size ranging from 15 to 20 nm. Fig. 5b shows the HRTEM micrograph of several nanoparticles of Co_3Mo_3C on MCM41 with the average dimensions of about 17 nm, as circled in the figure. According to the calculated average crystalline size, the active component exists as nano-scale single crystal dispersing on the MCM41 support. Meanwhile the magnified microregion of Fig. 5b, as shown in Fig. 5c, gives *d*-spacing values of 0.278 nm, which coincided with the (4 0 0) crystallographic plane of Co_3Mo_3C detected by XRD.

To apply the as-prepared materials in hydrotreating process, the HDS of DBT and 4,6-DMDBT and the HDN of 3-methylpyridine over Co_3Mo_3C/MCM41 were investigated, and the results were respectively plotted in Figs. 6 and 7. As shown in Fig. 6, increasing reaction temperature leads to an obvious increase in the HDS activities. At 593 K, the conversion of DBT and 4,6-DMDBT reaches 100% and 90.45%, respectively, suggesting an outstanding catalytic performance of the bimetallic carbides in deep HDS. HDN was selected as a test reaction to compare the catalytic activity of the supported catalyst prepared by our new method and conventional TPR method. The HDN activities of both catalysts are shown in Fig. 7. It is obvious that the conversion of 3-methylpyridine over Co_3Mo_3C/MCM41 catalyst prepared by HMT-based method (Fig. 7A) is higher than that prepared by TPR method (Fig. 7B). Thus, this new synthesis route has been proved to be effective for the preparation of bimetallic carbide catalyst. Since the synthesis process has been greatly simplified, such a simple HMT-based method possesses potential to be a general route to synthesize more active supported bimetallic carbide catalysts than the conventional TPR method.

To assess the nature, the specific activities of bimetallic carbide catalyst from the new method are calculated by the amount of converted probe molecule per Co_3Mo_3C molecule per hour. It is interesting to find that the specific activity of Co_3Mo_3C/MCM41 prepared by the new method is high up to 9.96 for HDN at 573 K, nearly 17 times higher than the sum of that for HDS at the same temperature (Table 1). To further understand the catalytic performance of the carbide material, it is essential to discuss on the structural and electrical properties of Co_3Mo_3C. Prior et al. [12] proposed, in the η-carbide M_3T_3X (M = Co and T = Mo in the current work), the M atoms network may be considered as metal-like in nature while T atoms network is more ionic due to the formation of T_6X octahedra and T-C bonding. In general, HDN reaction involves a dual-site mechanism, namely hydrogenation and C-N breaking. The kinetically rate-determining step in HDN of heterocyclic compounds over carbide catalyst is generally fixed in the hydrogenation of heterocyclic ring [7,16]. On the basis of this analysis, the metal-like Co atoms serve as the active sites where the activation of hydrogen takes place. Since in the active

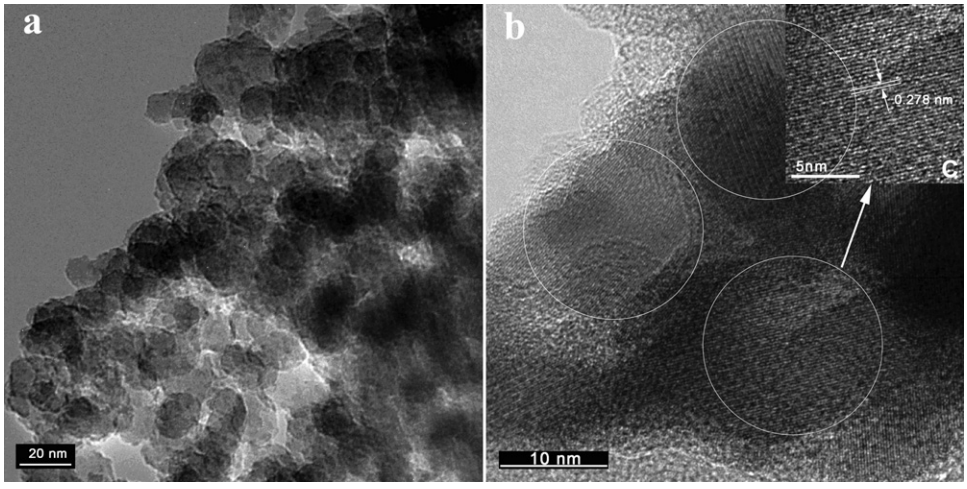

Fig. 5. The as-prepared Co_3Mo_3C/MCM41 catalyst. (a) TEM micrograph, (b) HRTEM micrograph of the Co_3Mo_3C nanoparticles and (c) Details of the circle area in B.

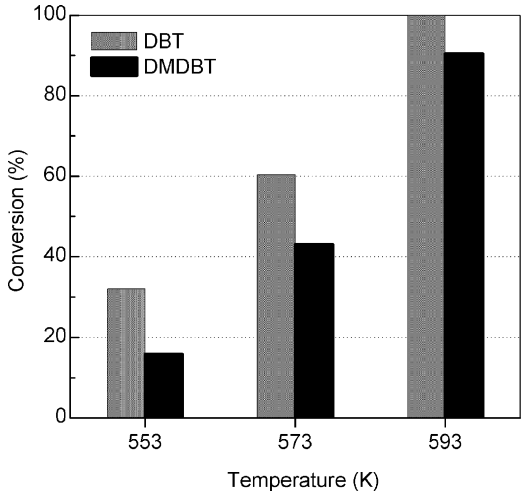

Fig. 6. The DBT and DMDBT HDS activities over the Co_3Mo_3C/MCM41 catalyst prepared by the thermal decomposition method.

component Co_3Mo_3C the metal-like Co sites remain intimately mixed with the active Mo sites, it makes it easy for the adsorbed hydrogen to transfer to the reactant molecules which are adsorbed on the Mo sites. This ensures the Co sites to be available for another adsorption-activation-transfer-adsorption cycle and results in a high hydrogenating activity in HDN.

However, in terms of the mechanism in HDS of DBT and 4,6-DMDBT, it is documented to proceed through two main parallel pathways, direct desulfurization (DDS) and hydrogenation (HG) [29–31]. According to the existing literatures, it is noted that for the molybdenum-based carbide catalyst the product of DDS route usually remains dominant [12,15,32–35]. Thus, the above described advantages should make less contribution to the HDS activity.

On the other hand, the interstitial carbon atoms modify the nature of the d bands of the parent metal, which increases the s–p electrons count and gives rise to the catalytic properties similar to that of group VIII noble metals [36]. In summary, this

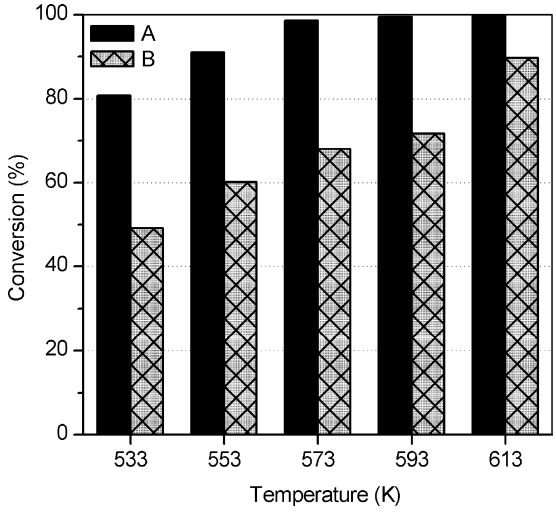

Fig. 7. The 3-methylpyridine HDN activities over the Co_3Mo_3C/MCM41 catalysts prepared by thermal decomposition method (A) and TPR method (B).

Table 1
The specific activities of the Co_3Mo_3C/MCM41 catalyst prepared by thermal decomposition in HDN and HDS

	HDN	HDS (DBT)	HDS (DMDBT)
Specific activity[a] (h^{-1})	9.96	0.42	0.17

[a] Converted probe molecule per Co_3Mo_3C molecule per hour at 573 K.

Co–Mo bimetallic carbide is believed to be the highly efficient catalyst for the hydrogen involved reactions, particularly for the reactions that hydrogenation is the kinetically rate-determining step.

4. Conclusion

In this work, Co_3Mo_3C and Co_6Mo_6C are prepared by the thermal decomposition of excess HMT-contained mixed-salt precursor, in which HMT acts as both molybdate ion ligand and carbon source. This simple synthetic method is proved to be effective to prepare MCM41 supported Co_3Mo_3C catalyst. HRTEM and BET surface area characterizations indicate that the active component Co_3Mo_3C display a uniform dispersion on the support. The as-prepared Co_3Mo_3C/MCM41 catalyst exhibits good activities in both HDS and HDN probe reactions, particularly in the latter. One proposal for explaining good performance of the carbide catalyst for HDN is that the material possesses special structural and electrical properties which benefit for the rate-determining step of hydrogenation in HDN.

Acknowledgements

The authors thank for the financial support of the National Natural Science Foundation of China (Grants 20403009), the Key Project of Chinese Ministry of Education (No. 105045), and Open Foundation of State Key Laboratory of Heavy Oil Processing.

References

[1] S.T. Oyama, Catal. Today 15 (1992) 179 (and references therein).
[2] J.-G. Choi, J.R. Brener, L.T. Thompson, J. Catal. 154 (1995) 33.
[3] A.P.E. York, J.B. Claridge, J. Brungs, S.C. Tsang, M.L.H. Green, Chem. Commun. (1997) 39.
[4] M.K. Neylon, S. Choi, H. Kwon, K.E. Curry, L.T. Thompson, Appl. Catal. A 183 (1999) 253.
[5] L. Delannoy, J.M. Giraudon, P. Granger, L. Leclercq, G. Leclercq, Catal. Today 59 (2000) 231.
[6] R. Kojima, K.-I. Aika, Appl. Catal. A 219 (2001) 141.
[7] A. Szymańsk, M. Lewandowski, C. Sayag, G. Djéga-Mariadassou, J. Catal. 218 (2003) 24.
[8] B. Diaz, S.J. Sawhill, D.H. Bale, R. Main, D.C. Phillips, S. Korlann, R. Self, M.E. Bussell, Catal. Today 86 (2003) 191.
[9] J.-M. Manoli, P.D. Costa, M. Brun, M. Vrinat, F. Maugé, C. Potvin, J. Catal. 221 (2004) 365.
[10] M.L. Pritchard, R.L. McCauley, B.N. Gallaher, W.J. Thomson, Appl. Catal. A 275 (2004) 213.
[11] W. Wu, Z. Wu, Z. Feng, P. Ying, Can Li, Phys. Chem. Chem. Phys. 6 (2004) 5596.
[12] P.D. Costa, J.-M. Manoli, C. Potvin, G. Djéga-Mariadassou, Catal. Today 107–108 (2005) 520.

[13] D.V. Potapenko, J.M. Horn, M.G. White, J. Catal. 236 (2005) 346.
[14] M. Nagai, K. Matsuda, J. Catal. 238 (2006) 489.
[15] M. Lewandowski, A. Szymańska-Kolasa, P.D. Costa, C. Sayag, Catal. Today 119 (2007) 31.
[16] A. Szymańska-Kolasa, M. Lewandowski, C. Sayag, D. Brodzki, G. Djéga-Mariadassou, Catal. Today 119 (2007) 35.
[17] J.M. Newsam, A.J. Jacobson, L.E. Mccandlish, R.S. Polizzotti, J. Solid State Chem. 75 (1988) 296.
[18] S. Korlann, B. Diaz, M.E. Bussell, Chem. Mater. 14 (2002) 4049.
[19] S. Alconchel, F. Sapiña, E. Martínez, Dalton Trans. (2004) 2463.
[20] T.-C. Xiao, A.P.E. York, H. Al-Megren, C.V. Williams, H.-T. Wang, M.L.H. Green, J. Catal. 202 (2001) 100.
[21] T.-C. Xiao, A.P.E. York, H. Al-Megren, J.B. Claridge, H.-t. Wang, M.L.H. Green, C. R. Acad. Sci. Paris, Série IIc, Chimie: Chem. 3 (2000) 451.
[22] H.A. Al-Megren, T. Xiao, S.L. Gonzalez-Cortesa, S.H. Al-Khowaiterb, M.L.H. Green, J. Mol. Catal. A 225 (2005) 143.
[23] C. Liang, W. Ma, Z. Feng, C. Li, Carbon 41 (2003) 1833.
[24] C. Liang, P. Ying, C. Li, Chem. Mater. 14 (2002) 3148.
[25] C. Liang, F. Tian, Z. Li, Z. Feng, Z. Wei, C. Li, Chem. Mater. 15 (2003) 4846.
[26] P. Afanasiev, Inorg. Chem. 41 (2002) 5317.
[27] H. Wang, W. Li, M. Zhang, Chem. Mater. 17 (2005) 3262.
[28] H.-M. Wang, X.-H. Wang, M.-H. Zhang, X.-Y. Du, W. Li, K.-Y. Tao, Chem. Mater. 19 (2007) 1801.
[29] M. Houalla, N.K. Nag, A.V. Sapre, D.H. Broderick, B.C. Gates, AIChE J. 24 (1978) 1015.
[30] N. Kagami, B.M. Vogelaar, A.D. van Langeveld, J.A. Moulijn, Appl. Catal. A 293 (2005) 11.
[31] M.S. Rana, R. Navarro, J. Leglise, Catal. Today 98 (2004) 67.
[32] L.A. Santillán-Vallejo, J.A. Melo-Banda, A.I.R. de la Torre, G. Sandoval-Robles, J.M. Domínguez, A. Montesinos-Castellanos, J.A. de los Reyes-Heredia, Catal. Today 109 (2005) 33.
[33] A. Hynaux, C. Sayag, S. Suppan, J. Trawczynski, M. Lewandowski, A. Szymanska-Kolasa, G. Djéga-Mariadassou, Appl. Catal. B 72 (2006) 62.
[34] A. Hynaux, C. Sayag, S. Suppan, J. Trawczynski, M. Lewandowski, A. Szymanska-Kolasa, G. Djéga-Mariadassou, Catal. Today 119 (2007) 3.
[35] A. Szymańska-Kolasa, M. Lewandowski, C. Sayag, G. Djéga-Mariadassou, Catal. Today 119 (2007) 7.
[36] J.G. Chen, Chem. Rev. 96 (1996) 1477.